A Coupled-Cluster Analysis of the Electronic Excited States in Aminobenzonitriles

Andreas B. J. Parusel* and Gottfried Köhler

Institute for Theoretical Chemistry and Radiation Chemistry, University of Vienna, Althanstrasse 14, 1090 Vienna, Austria, and Austrian Society for Aerospace Medicine—Institute for Space Biophysics, Lustkandlgasse 52/3, 1090 Vienna, Austria

Marcel Nooijen†

Chemistry Department, Princeton University, Princeton, New Jersey 08544

Received: November 6, 1998; In Final Form: February 22, 1999

The excited states of 4-(*N*,*N*-dimethylamino)benzonitrile (DMABN) and 4-aminobenzonitrile (ABN) are characterized by the *similarity transformed equation-of-motion coupled-cluster method with single and double excitations* (STEOM-CCSD). The long wavelength band of DMABN is assigned by STEOM-CCSD to an emission of a geometrically relaxed twisted intramolecular charge transfer (TICT) state. In contrast, no lowering in total energy upon twisting is found in ABN. The different behavior of the TICT states in ABN and DMABN can quite clearly be understood from the behavior upon twisting of the correlated ionization potentials and electron affinities from IP/EA-EOM-CCSD results that are obtained as a side product of STEOM-CCSD calculations. Inclusion of electron correlation is found to be crucial however, as the effect is largely lost at the Hartree−Fock (Koopmans') level of accuracy. The STEOM-CCSD results are similar to results from DFT/SCI calculations. In general they also agree well with results from previous CASPT2 calculations and experimental data, where available. The crucial behavior of the energy of the TICT states upon rotation of the amino group in ABN and DMABN differs markedly however, between STEOM-CCSD and CASPT2. Whereas in STEOM-CCSD upon twisting we find the expected lowering for the TICT state in DMABN and rise in energy for ABN, this is not the case in CASPT2. Previous benchmarks indicate that CASPT2 may have difficulties describing differential dynamical correlation associated with transitions from lone pair orbitals, and we think therefore that the results at the STEOM-CCSD and DFT/SCI levels may be more accurate for this aspect of the problem.

1. Introduction

Several organic donor-acceptor substituted compounds exhibit the phenomenon of dual fluorescence in polar solvents. In addition to the so-called normal fluorescence from the solvent relaxed primary excited state, a second, red-shifted emission band is observed for these systems. This strongly solvent dependent anomalous fluorescence is assigned to an emission from a highly polar intramolecular charge transfer state. This dual fluorescence was first found for 4-(*N*,*N*-dimethylamino)-benzonitrile (DMABN, see Figure 1) in 1959[1] and was investigated for a wide class of related donor-acceptor systems (for a review, see, e.g., refs 2 and 3). Several models for the explanation of this unusual behavior have been subsequently proposed, but the photophysics of this phenomenon has most frequently been discussed within the twisted intramolecular charge transfer (TICT) model by Z. R. Grabowski and co-workers.[4,5] In this model, the highly polar charge transfer excited state is formed by internal twisting of the donor (dimethylamino subunit) relatively to the acceptor (benzonitrile subunit) in the excited state. Nevertheless, several other models, as complexation or formation of exciplexes with the solvent[6−8] or solvent-induced vibronic coupling between the energetically close lying first singlet states,[9,10] are still discussed as possible explanations.

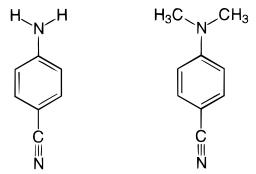

Figure 1. Structures of ABN (left) and DMABN (right).

4-Aminobenzonitrile (ABN, see Figure 1), having a similar structure as DMABN, shows no evidence of dual fluorescence even in strongly polar environments.[9−11] This absence of a charge transfer emission is attributed to an increased energy gap between the first and second excited state[9−11] and due to the lower donor strength of the amino group.[3]

Numerous theoretical calculations have been carried out for these molecules, from early PPP calculations[4] in 1979 to recently published CASPT2[12−14] and DFT/SCI[15] calculations. CASPT2 as well as MRD-CI require a careful selection of active orbitals and it may be difficult to characterize the excited states in a consistent manner. In contrast, the so-called equation-of-motion coupled cluster method with single and double excitations (EOM-CCSD)[16−18] does not need such considerations; solely the selected basis set and rank of the excitation level have to be chosen. However, the computational costs of EOM-CCSD are quite demanding, as each excited state is an eigenvector of a diagonalization problem over the space of single and double excitations. In addition a triples correction may be required to

* Corresponding author. Fax: +43 1 31336 790. E-mail: andreas@majestix.msp.univie.ac.at.
† Fax: +1 609 258 6746. E-mail: nooijen@princeton.edu.

10.1021/jp984346w CCC: $18.00
Published on Web 05/05/1999

attain high accuracy, in particular for valence excited states. Recently EOM-CCSD and EOM-CCSD($\tilde{T}$) calculations of the excitation energies of benzene and the azabenzenes[19] have been published and within the context of EOM-CCSD these can be considered as large organic molecules. In 1997 a newly developed method for excited states was presented.[20,21] The so-called similarity transformed equation-of-motion coupled-cluster theory (STEOM-CC) uses a double similarity transformation of the second quantized Hamiltonian. The final transformed Hamiltonian is diagonalized over the space of singly excited determinants only. Thus, a large number of excited states can be calculated without extensive computational costs. It has been shown in recent studies on free base porphin[22,23] that the STEOM-CCSD method can be applied to large organic molecules, and the results have been found in good agreement with experiment.

In the current work, a detailed study of the first excited states of ABN and DMABN is presented for the planar and twisted (i.e., decoupled) C_{2v} conformation. DFT optimized ground state geometries are followed by a STEOM-CCSD investigation of the excited state properties. Also the low lying ionized and attached states of ABN and DMABN are determined in order to gain insight in the difference between ABN and DMABN in the context of the process of dual fluorescence.

2. Computational Details

In a previous work the DFT optimized geometries of DMABN have been shown to be superior to those derived by Hartree−Fock ab initio and AM1 semiempirical methods.[15] A direct comparison of basis sets shows that a valence double zeta basis set including polarization functions is adequate. Only small improvements in excited state properties can be achieved by the use of larger basis sets, at least at the DFT/SCI level. We employ the cc-pVDZ Dunning's correlation basis set (double-ζ; C,N:[3s2p1d], H:[2s1p]).[24−26] The ground state optimizations are performed with the exchange correlation functional of Becke, and Lee, Yang, and Parr, in its hybrid form, i.e., with inclusion of nonlocal corrections and some portion of exact Hartree−Fock exchange (B3LYP)[27,28] as implemented the GAUSSIAN94 program package.[29] For the investigation of the TICT model, a second geometry with an amino group perpendicular to the benzonitrile moiety (i.e., twisting angle of 90°) is optimized for ABN and DMABN. C_{2v} symmetry is retained for both compounds and all conformations.

All excited state calculations are performed with the ACESII program system.[30,31] Excitation energies and excited state properties are computed with the similarity transformed equation-of-motion coupled-cluster method including single and double excitations (STEOM-CCSD).[20,21] The basic idea underlying STEOM is to transform all important matrix elements of the Hamiltonian to zero that couple from singly excited to more highly excited determinants. In practice a STEOM calculation proceeds in a number of steps. The first step is a CCSD calculation on the ground state. This is the rate determining step in the calculation. Subsequently the so-called EOM Hamiltonian $\bar{H} = e^{-T}He^{T}$ is formed and diagonalized over the *1h,2hp* space (an IP-EOMCC calculation[18,32,33]) to yield the principal ionization energies of the system. In addition electron affinities are obtained in an EA-EOM-CCSD[34] calculation by diagonalizing over the *1p, 2p1h* configurations. These latter states need not correspond to bound anionic states. They may be artificial, very much like the virtual orbital energies themselves. In the IP-EOM and EA-EOM steps a selection of principal cationic and anionic states is made, and this constitutes the active space in a STEOM-CCSD calculation. The active space in STEOM is associated with dynamical correlation effects and is quite large, typically including something like 10 occupied and up to 30 virtual orbitals. The selection of the active space is not very critical beyond a certain level. From the EOMCC eigenvectors associated with the IP's and EA's a second transformation is extracted. The doubly transformed STEOM Hamiltonian *G* satisfies the desirable decoupling conditions and is diagonalized over the space of singly excited configurations to obtain the predominantly singly excited states of the system. Implicitly, higher order excitations are also included in STEOM.[21] In particular, STEOM-CCSD includes a triple correction when compared to EOM-CCSD. For the present purpose a major advantage of the STEOM approach is that as a byproduct we obtain ionization potentials and electron affinities of the system at the same level of accuracy as the excitation energies and they are found to correlate directly to the phenomenon of dual fluorescence, and as such provide an easy explanation for the difference between ABN and DMABN.

3. Results

3.1. Frontier Orbitals Characterization of ABN and DMABN. The correlated IP-EOMCC[32,33] and EA-EOMCC[34] methods have been established to give quite reliable results for ionization potentials and electron affinities.[18,20] This is true in particular for molecules having lone pairs, where Koopmans' theorem is often deficient.[20,22,23] We will use the IP/EA-EOMCC results to understand the difference between ABN and DMABN upon twisting. In Figure 2 the correlated ionization/attachment energies of relevant anionic states (corresponding to π^* orbitals) and cationic states (corresponding to occupied frontier orbitals) are plotted as a function of geometry. In addition we have indicated the corresponding molecular orbitals at the planar and twisted geometries.

The LUMO and LUMO+1, of B_1 and A_2 symmetry, respectively, have π^* character and stabilize along the twisting coordinate. The LUMO+1 is delocalized over the benzyl moiety, and only a slight decrease of the energy is found for this orbital. The LUMO has a small antibonding lobe at the amino nitrogen at the planar geometry. This antibonding character is absent at the twisted geometry, and this gives rise to the observed stabilization of the LUMO at the twisted geometry for both ABN and DMABN. Results at the HF MO level are qualitatively similar to the correlated EA-EOMCC level, although at the HF level the attachment energies are about 1 eV higher. Also at the semi-empirical level the characterization of the virtual orbitals is essentially correct.[35]

The situation for the occupied orbitals is more intriguing. As seen from Figures 2a,b the $\pi(A_2)$ orbital has no amino character and it is therefore insensitive to twisting of the amino group. Furthermore it has almost the same orbital energy in ABN and DMABN. The remaining two frontier orbitals are more complicated. The situation is easiest to analyze at the twisted geometry since they then fall in different symmetries. The HOMO has nitrogen lone pair character in both ABN and DMABN. However, the ionization potential for DMABN is substantially lower than in ABN. This is due to the presence of the electron donating methyl groups on the amino nitrogen which stabilize the cation and, hence, lower the ionization potential in DMABN compared to ABN. At the twisted geometry the other frontier orbitals of B-symmetry, the HOMO-1, has predominantly π character with little amino contribution. For DMABN the amino lone pair IP (HOMO) is well separated from the others. For ABN, however, all three frontier orbitals are very close in energy.

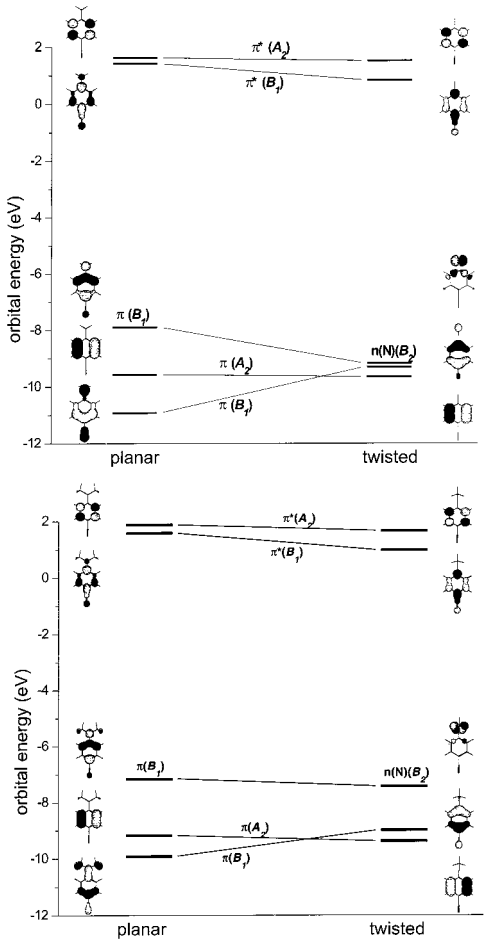

Figure 2. Correlation diagram (frontier orbital region) of (top) ABN and (bottom) DMABN as a function of the twist angle in notation of C_{2v} symmetry.

Upon rotating the amino group to the planar geometry, the lone pair on nitrogen becomes part of the π system and strong mixing occurs between the orbitals/states of B symmetry. Both frontier orbitals have nitrogen lone pair character, and at the planar geometry the symmetry of both orbitals is B_1. For ABN this results in a large splitting, due to the closeness of the levels at the twisted geometry. The HOMO goes up upon reaching the planar geometry, while the other B_1 orbital goes down appreciably and becomes the HOMO-2 at the planar geometry. For DMABN the effect of rotation is far less because the separation of the states is larger at the twisted geometry. Hence the HOMO in DMABN at the planar geometry is only slightly higher than at the twisted geometry.

As mentioned before, the Hartree−Fock method, or Koopmans' theorem, is often deficient when describing the relative ordering and stability of nitrogen lone pair orbitals in a conjugated π system.[20,22,23] This is evidenced again in the present calculations. At the HF level the lone pair orbital is not the HOMO at the twisted geometries, but lies inside the π manifold. This is very different at the correlated level. Only for ABN at the twisted geometry is the nitrogen lone pair IP close to the other correlated IPs. Even then it is still the lowest cationic state, while it is lying far deeper at the Koopmans' level. From Tables 1 and 2 the orbitals that have nitrogen lone pair character can be characterized by the fact that the correlated IP's are very different from the Koopmans' values (close to a 2 eV difference at the twisted geometry, more like 1 eV at the planar geometry). In contrast ionization potentials corresponding to orbitals having purely π character vary little upon inclusion of correlation. As

TABLE 1: Ionization Potentials and Electron Attachment Energies (in eV) of Planar ABN and DMABN

	ABN		DMABN		
orbital	Koopmans	EOM-CCSD	Koopmans	EOM-CCSD	exptl[44]
			Ionization Potentials		
$\pi(B_1)$	8.33	7.89	8.07	7.32	7.9
$\pi(A_2)$	9.90	9.57	9.77	9.34	9.6
$\pi(B_1)$	11.97	10.92	11.28	10.08	10.2
			Electron Attachment		
$\pi^*(B_1)$	2.67	1.42	2.62	1.41	
$\pi^*(A_2)$	2.89	1.62	2.99	1.71	

TABLE 2: Ionization Potentials and Electron Attachment Energies (in eV) of Twisted ABN and DMABN

	ABN		DMABN	
orbital	Koopmans	EOM-CCSD	Koopmans	EOM-CCSD
		Ionization Potentials		
$n(N)(B_2)$	10.97	9.17	9.55	7.59
$\pi(A_2)$	9.80	9.64	9.78	9.54
$\pi(B_1)$	9.48	9.30	9.43	9.15
		Electron Attachment		
$\pi^*(B_1)$	2.03	0.84	2.03	0.81
$\pi^*(A_2)$	2.82	1.52	2.82	1.50

a result the HF MO energies do not provide a reliable picture of the ordering and changes of the cationic states upon twisting. There is no doubt that the IP-EOMCC method provides the correct picture. The situation at the DFT level is similar to HF, and also here the description is not quite correct, though improved compared to HF, as no orbital crossing occurs.[15] Also the semiempirical level is slightly deficient but far better than Hartree−Fock.[35] Comparing to experiment the IP-EOMCC method provides reasonable results, although the HOMO energy at the planar geometry is a little low. It is known from experience that adding a second polarization function tends to increase the first IP significantly, which would improve the agreement with experiment.

3.2. Vertical Excitation Spectra. In Table 3 STEOM-CCSD results are presented for the low-lying states of ABN and DMABN at their planar geometry. The spectral features of ABN and DMABN are of course very similar. The first excited state, at about 4.20 eV, has B_2 symmetry and is only a weakly allowed transition. The most intense transition is into the second excited state around 5 eV. This state has A_1 symmetry and is a charge transfer state as evidenced by the large change in dipole moment, compared to the ground state. The dipole moments tend to be a little larger in DMABN than in ABN, and this can be understood from the electron donating character of the methyl groups. Upon excitation the dipole moments of all states increase. This is due to the fact that the $\pi^*(B_1)$ orbital is more localized towards the cyano group than the $\pi(B_1)$ orbital. In Table 3 also the low lying triplet states are included. Often one finds that singlet and triplet states come in matching pairs, which are similar in excitation character, although they can differ substantially in excitation energy, due to the effects of different exchange interactions between open-shell orbitals in the singlet and triplet states. However, this matching is rather poor in ABN and DMABN, as is clear from the excitation character in the various states as indicated in Table 3. In particular we do not find a low lying triplet state that has significant charge transfer character. In fact no such state is found in the range up to 7 eV. Together with the orbital plots and the state character this indicates that the charge transfer excitation involves a rather subtle redistribution of charge that is not straightforwardly associated with excitation from amino- to benzonitrile moiety.

TABLE 3: Total Energies (*E*, in au), Vertical Excitation Energies (Δ*E*, in eV), Oscillator Strengths (*f*), and Dipole Moments (*μ*, in debye) of Planar ABN and DMABN Excited States along with their Weights (greater than 5%) in C_{2v} Symmetry

	E	Δ*E*	*f*	*μ*	assignment
ABN					
S_0	−378.771 550 3			6.81	
1^1B_2	−378.614 798 7	4.27	0.0192	7.61	$\pi(B_1) \rightarrow \pi^*(A_2)$ 74%
					$\pi(A_2) \rightarrow \pi^*(B_1)$ 25%
2^1A_1	−378.582 861 5	5.13	0.5511	11.61	$\pi(B_1) \rightarrow \pi^*(B_1)$ 90%
1^3A_1	−378.651 959 2	3.25		7.84	$\pi(B_1) \rightarrow \pi^*(B_1)$ 79%
					$\pi(A_2) \rightarrow \pi^*(A_2)$ 14%
1^3B_2	−378.620 615 9	4.11		8.79	$\pi(B_1) \rightarrow \pi^*(A_2)$ 92%
DMABN					
S_0	−457.061 456 4			7.50	
1^1B_2	−456.908 893 4	4.15	0.0216	9.16	$\pi(B_1) \rightarrow \pi^*(A_2)$ 78%
					$\pi(A_2) \rightarrow \pi^*(B_1)$ 19%
2^1A_1	−456.887 787 1	4.73	0.6577	13.54	$\pi(B_1) \rightarrow \pi^*(B_1)$ 90%
1^3A_1	−456.944 543 6	3.18		9.14	$\pi(B_1) \rightarrow \pi^*(B_1)$ 82%
					$\pi(A_2) \rightarrow \pi^*(A_2)$ 10%
1^3B_2	−456.915 453 9	3.97		10.49	$\pi(B_1) \rightarrow \pi^*(A_2)$ 95%

TABLE 4 : Total Energies (*E*, in au), Vertical Excitation Energies (Δ*E*, in eV), Oscillator Strengths (*f*), and Dipole Moments (*μ*, in debye) of Excited States along with their Weights (greater than 5%) of Twisted ABN and DMABN in C_{2v} Symmetry

	E	Δ*E*	*f*	*μ*	assignment
ABN					
S_0	−378.757 619 8			5.06	
1^1B_2	−378.589 230 1	4.58	0.0030	5.34	$\pi(B_1) \rightarrow \pi^*(A_2)$ 44%
					$\pi(A_2) \rightarrow \pi^*(B_1)$ 54%
1^1A_2	−378.571 502 0	5.06	0.0000	14.54	$n(B_2) \rightarrow \pi^*(B_1)$ 92%
					$n(B_2) \rightarrow \pi^*(2B_1)$ 6%
1^3A_1	−378.634 773 1	3.34		5.35	$\pi(B_1) \rightarrow \pi^*(B_1)$ 67%
					$\pi(A_2) \rightarrow \pi^*(A_2)$ 26%
1^3B_2	−378.588 259 5	4.61		5.89	$\pi(B_1) \rightarrow \pi^*(A_2)$ 32%
					$\pi(A_2) \rightarrow \pi^*(B_1)$ 67%
1^3A_2	−378.569 613 9	5.06		15.22	$n(B_2) \rightarrow \pi^*(B_1)$ 94%
DMABN					
S_0	−457.045 136 3			5.19	
1^1B_2	−456.877 933 5	4.55	0.0030	5.41	$\pi(B_1) \rightarrow \pi^*(A_2)$ 47%
					$\pi(A_2) \rightarrow \pi^*(B_1)$ 52%
1^1A_2	−456.898 191 1	3.99	0.0000	16.28	$n(B_2) \rightarrow \pi^*(B_1)$ 100%
1^3A_1	−456.924 174 5	3.29		5.49	$\pi(B_1) \rightarrow \pi^*(B_1)$ 58%
					$\pi(A_2) \rightarrow \pi^*(A_2)$ 36%
1^3A_2	−456.896 351 4	4.05		16.97	$n(B_2) \rightarrow \pi^*(B_1)$ 100%
1^3B_2	−456.877 278 6	4.57		5.99	$\pi(A_2) \rightarrow \pi^*(B_1)$ 58%
					$\pi(B_2) \rightarrow \pi^*(A_2)$ 40%

In Table 4 total energies, excitation energies, dipole moments, and transition moments are included for ABN and DMABN at the twisted geometry. Due to the fact that the nitrogen lone pair is completely associated with the orbitals of B_2 symmetry a very simple picture emerges. The pure $\pi \rightarrow \pi^*$ excitations have very similar excitation energies in ABN and DMABN. The influence of the methyl groups is negligible. On the other hand, the charge transfer state can be fully characterized as $n \rightarrow \pi^*$ and differs appreciably between ABN (5.06 eV) and DMABN (3.99 eV). This difference in excitation energy (1.07 eV) correlates to the difference in correlated ionization potentials of ABN and DMABN (1.58 eV). Moreover, the excitation energy of the charge transfer state in DMABN is substantially lower in DMABN at the twisted geometry than at the planar geometry (0.78 eV). This difference is mainly due to the decrease in attachment energy of the $\pi^*(B_1)$ orbital upon twisting, as the IP of DMABN is fairly invariant. In contrast in ABN the IP corresponding to the nitrogen lone pair lowers upon twisting and as a result the $n \rightarrow \pi^*$ excitation energy is almost constant. The charge transfer state at the twisted geometry has a very large dipole moment, and moreover the singlet and triplet states are very similar in character and energy. This indicates that the orbitals involved in the excitation are separated in space, and interact only slightly. The $n \rightarrow \pi^*$ transition is forbidden by symmetry, so upon twisting the CT state evolves from being strongly allowed to forbidden.

The present STEOM-CCSD results are compared in Tables 5 and 6 with previous theoretical results. We have included CASPT2 results from ref 12 and DFT/SCI results from ref 15. The DFT/SCI results for ABN were obtained as part of this work.

Let us consider first the planar geometry. For ABN, the first excited state is of B_2 symmetry with a STEOM-CCSD excitation energy of 4.27 eV, 4.3 by DFT/SCI and 4.01 eV according to CASPT2 theory. This number is in good agreement with experiment, where an excitation energy of 4.15 eV is obtained by molecular free jet experiments[39] and above 4.0 eV by UV spectroscopy.[9] The absorption is calculated with an oscillator strength of 0.0192 (CASPT2: 0.004) and observed in UV spectroscopy only as a very weak shoulder. The main absorption, as observed in experiment, occurs into the second excited state. This corresponds to a calculated oscillator strength of 0.5511 (CASPT2: 0.361). The $2A_1$ state is of charge transfer character with a STEOM excitation energy of 5.13 eV compared to 4.74 eV as obtained by experiments,[9] 5.0 eV by DFT/SCI, and 4.44 eV by CASPT2. The calculated dipole moment of the second excited state is 11.61 D (CASPT2: 12.42 D) and corresponds to a highly dipolar electron distribution. It is clear that the CT excitation that involves major rearrangement of the electron

distribution is hard to calculate. STEOM-CCSD and DFT/SCI agree remarkably well, while CASPT2 differs substantially. The experimental value is somewhere in between.

For DMABN at the planar geometry STEOM excitation energies of 4.15 and 4.73 eV are computed for the first and second excited state (CASPT2: 4.05 and 4.41 eV. DFT/SCI: 4.05 and 4.56 eV). The first excitation energy is in good agreement with the experimental data of 4.00 eV obtained by jet experiments[40] and UV spectroscopy,[9] while the dominant absorption occurs into the second excited state at 4.42 eV.[9] The CASPT2 results are in better agreement with experiment than our STEOM-CCSD computations, although we note that comparing vertical excitation energies with experimental band maxima involves severe approximations, certainly in solution. From experience we know that STEOM-CCSD results saturate a little slower with improving the basis set than CASPT2 or DFT/SCI. An improved basis set would tend to lower STEOM excitation energies, leading to improved overall agreement. The oscillator strengths of 0.0216 (S_1) and 0.6577 (S_2) are comparable to experiment (0.04 (S_1) and 0.33 (S_2))[4,10,41] and to the CASPT2 results (0.010 (S_1) and 0.416 (S_2)). The dipole moment is determined by experiment in the range between 5.8 D (electrooptical measurements) and 11.4 D (solvatochromic results).[42] The reliable transient electron loss method yields 9.11 D,[6] which is in excellent agreement with the STEOM-CCSD value of 9.16 D. The CASPT2 dipole moment of 7.6 D[12] is located at the lower, and the DFT/SCI value of 11.5 D[15] at the upper limit, of the experimental range. In general, also the efficient DFT/SCI method yields comparable results: Both the exitation energies (4.05 eV (S_1) and 4.56 eV (S_2)) and oscillator strengths (0.027 (S_1) and 0.658 (S_2)) are of high quality.

At the twisted geometry we find major differences between our results and CASPT2, especially for ABN. The excitation energy of the 2A charge transfer state differs by 1.24 eV between STEOM-CCSD and CASPT2. So, whereas in STEOM-CCSD the excitation energy to this state for ABN is more or less invariant with respect to twisting, in CASPT2 there is a significant decrease in excitation energy. DFT/SCI is intermediate between the two results, giving an excitation energy that lies 0.5 eV below STEOM-CCSD. Unfortunately there are no experimental numbers to compare to for ABN. However, in this context, previous studies of the azabenzenes[19] may be particularly relevant. Del Bene, Watts, and Bartlett carried out EOM-CCSD($\tilde{T}$) calculations for benzene and a series of azabenzenes and compared their results to CASPT2 results. Whereas the results corresponding to $\pi \rightarrow \pi^*$ excitations were very good for either method, results for the $n \rightarrow \pi^*$ excitations often showed significant deviations, and the EOM-CCSD results were found to agree substantially better with experiment. CASPT2 results were found to deviate appreciably, usually falling below EOM-CCSD($\tilde{T}$) results and experiment. Recently, one of us (M. Nooijen), applied the STEOM-CCSD method to this problem and got very nice agreement with EOM-CCSD($\tilde{T}$) for the excitations involving nitrogen lone pair orbitals. In addition adiabatic excitation energies were calculated using STEOM-CCSD at CIS based geometries for the excited states and results were typically accurate to within 0.1 eV for the low lying states, involving excitation from the nitrogen lone pair. Let us note here that a comparison of adiabatic excitation energies is far less ambiguous than a comparison of vertical excitation energies that involve a number of (sometimes severe) approximations. From this experience we have considerable confidence in STEOM-CCSD, and, moreover, the study on the azabenzenes points out potential problems with CASPT2: the importance of dynamical correlation for nitrogen lone pair orbitals is indicated by the deficiency of Koopmans' theorem. On the other hand the main source of error in the present STEOM-CCSD calculation is probably the limited size of basis set used, but increasing the basis set is unlikely to decrease the excitation energies by more than 0.3 eV. The $\pi \rightarrow \pi^*$ in twisted ABN exitation also differs, but this is within the usual error margins. Again DFT/SCI tends to be closer to STEOM-CCSD than to CASPT2.

For DMABN the CASPT2 fluorescence energy (3.94 eV) of the twisted 2A state is virtually identical to our results (3.99 eV) compared to an experimental fluorescence energy of 3.2 eV. The DFT/SCI method[15] gives the best results for a not completely decoupled geometry (i.e., at a twisting angle of 60°) when comparing to experimental data: The long wavelength band is computed to be 3.35 eV. The fluorescence energy would be reduced further if the geometry used would be optimized for the fluorescing excited state at the twisted geometry. In the present calculations (and also the CASPT2 calculations) the geometry is optimized for the ground state. From the CASPT2 results a reduction of the excitation energy by 0.2 eV was obtained upon a wagging distortion of the amino group. A sizeable reduction of the fluorescence energy appears possible upon relaxation of the excited state geometry (which will simultaneously raise the ground state energy), and inclusion of solvent effects. This also implies, however, that DFT/SCI is likely to underestimate the fluorescence energy if the proper geometry is used and solvent effects are considered.

In Tables 3 and 4 also the excitation energies and dipole moments of the lowest excited triplet states are given. The first triplet state energy of DMABN in its ground state geometry of 3.18 eV is found in fair agreement with the experimental value of 2.81 eV[36] as measured in glassy ethanol. The energy of this benzenoid-like state of low polarity is thus better represented by our computation than by the CASPT2 T_1 energy of 3.66 eV.[12] The increased $\pi(A_2)\ \pi^*(A_2)$ contribution in the triplet $^3A_1$ compared to the $^1A_1$ state leads to less charge transfer character as can be seen by the smaller dipole moment of 7.84 D (ABN) and 9.14 D (DMABN). Both for ABN and DMABN a slight increase in the lowest triplet excitation energy results upon rotation and no evidence of an increased charge transfer character is found for them. The dipole moments for both triplet states of $^3A_1$ and $^3B_2$ symmetry in fact decrease with the twisting angle. The second excited triplet state of twisted DMABN (1^3A_2, see Table 4) does have a significant charge transfer character ($\mu(^3\text{TICT}) = 16.97$ D) and is nearly degenerate to the singlet TICT state ($\Delta E(^1\text{TICT} - {}^3\text{TICT}) = 0.06$ eV). This behavior is consistent with a charge transfer excitation when the orbitals involved do not overlap, and consequently the exchange integral that determines the singlet−triplet splitting is very small. A similar state is found in twisted ABN, and it is again degenerate with the singlet TICT state. In contrast, at the planar geometry the charge transfer triplet state corresponding to the singlet 1^1A_1 CT state, that would evolve into the TICT triplet state upon twisting, is not found for either ABN or DMABN. This shows that at the planar geometry, due to the conjugation of the nitrogen lone pair orbital and the π electron frame, the CT state does not consist of an excitation between two non-interacting orbitals. There is an appreciable exchange integral and a severe mixing with other configurations that obscure a potential triplet CT state at the planar geometry.

3.3. Interpretation of Fluorescence Spectra. The first type of fluorescence in both ABN and DMABN occurs from the planar conformation. Absorption at the planar geometry pre-

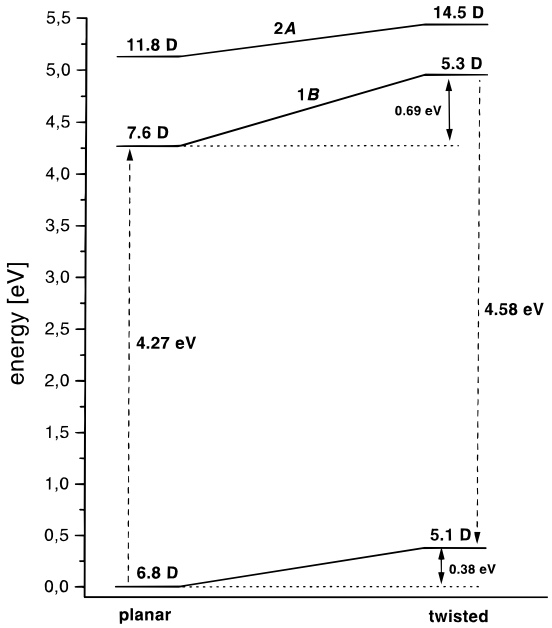

Figure 3. Potential energy (energy relative to the C_{2v} minimum of the ground state) of planar and twisted ABN.

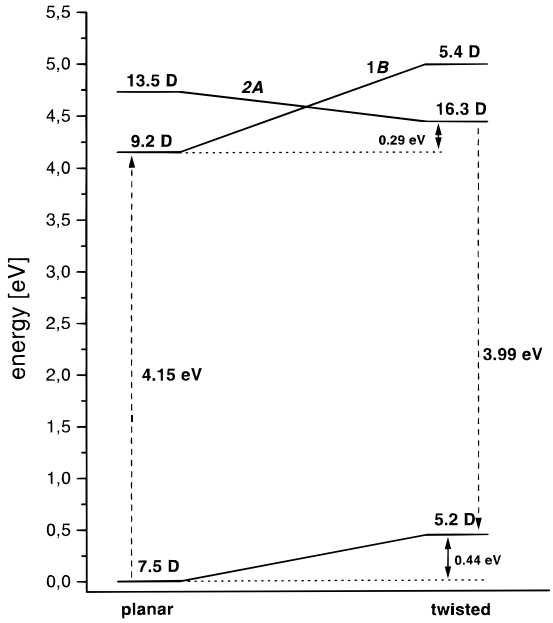

Figure 4. Potential energy (energy relative to the C_{2v} minimum of the ground state) of planar and twisted DMABN.

dominantly populates the strongly allowed S_2 state which undergoes a radiationless transition to the S_1 state, which relaxes and fluoresces. The second type of fluorescence is our prime interest, and it requires the twisting of the amino group in the excited state after absorption. The variation of the lowest singlet state energy as a function of the twist angle is shown for ABN in Figure 3 and for DMABN in Figure 4. The results obtained for excitation energies, dipole moments, and oscillator strengths for ABN and DMABN are presented in Tables 3−6.

Inspection of the potential curves along the twisting path shows an increase in energy for both the ground state and first excited state of B symmetry. The twisting barrier in the electronic ground state is calculated to be approximately 0.4 eV (ABN: 0.38 eV. DMABN: 0.44 eV.) and goes along with a decrease in dipole moment of approximately 2.5 D ($\mu_{\text{planar}} - \mu_{\text{twisted}}$ amounts to −2.7 D for ABN and −2.3 D for DMABN).

The excited state of B symmetry raises more sharply in energy than the ground state, implying a raise in excitation energy upon twisting. STEOM-CCSD yields a raise in total energy in the B state of 0.69 eV (ABN) and 0.84 eV (DMABN). The evolution in dipole moment corresponds to the situation for the electronic ground state. The resulting changes are qualitatively of the same magnitude in both ground and excited state. The excitation to the first state of B symmetry is characterized for both planar and twisted conformation by a benzene type $\pi\pi^*$ transition with decreasing contribution of the amino group, thus explaining the decreasing dipole moment. The contribution of the second $\pi \rightarrow \pi^*$ determinant increases with increasing twist angles. At the perpendicular geometry, almost an equal mixing (approximately 50% for both one-electron transitions involved) is observed. All oscillator strengths for the excitation into the B state are very small.

Analyzing further the charge-transfer 2A state we see that the dipole moment increases upon twisting in both ABN (from 11.8−14.5 D) and DMABN (from 13.5−16.3 D). The change in oscillator strength clearly reflects the change in the nature of the 2A state. The Franck−Condon allowed character at planar conformation corresponds to a large magnitude of the oscillator strength which decreases along the twisting coordinate and finally becomes zero for completely decoupled subunits, thus indicating a forbidden $n \rightarrow \pi^*$ transition. The symmetry of the 2A state, A_1 at planar geometry, becomes A_2 at twisted conformations due to the different orbital symmetry of the donor orbital involved. The total energy of the highly polar 2A charge transfer state behaves quite differently in ABN vs DMABN. For ABN the energy of the 2A state increases by about 0.31 eV in going from the planar to the twisted conformation, while a significant stabilization in energy is calculated for DMABN (−0.28 eV). Therefore, a diminished difference in energy between the first excited state and ground state is found for DMABN ($\Delta E = 3.99$ eV), while the excitation energy difference in ABN is more or less constant. The situation as calculated by STEOM-CCSD is markedly different in the CASPT2 calculations. In the CASPT2 calculation the total energy of the charge transfer state in ABN *decreases* by 0.25 upon twisting while the CASPT2 energy for the 2A state in DMABN is more or less constant. As discussed before, we hold the STEOM-CCSD picture to be the more accurate.

How do the STEOM-CCSD data explain the dual fluorescence, seen only in polar media for DMABN? Our calculations refer to the gas phase situation and, in agreement with experiment, it is predicted that no dual fluorescence occurs in either ABN or DMABN. In ABN the relevant 2A state increases in energy upon twisting. In DMABN the energy of the 2A state is lowered, and it does become the lowest state at the twisted geometry. However, the energy of the partially relaxed 2A state is still higher than the energy of the 1B state at the planar geometry, and only single fluorescence from the relaxed 1B state is expected. There are remaining uncertainties concerning the gas phase data as a complete calculation would involve the optimization of the excited state geometries and inclusion of zero point frequencies.

Upon solution in polar media the situation would change. The increase in dipole moment upon twisting will lower the energy of the 2A state due to interactions with the solvent. This true for both ABN and DMABN. In DMABN the effect can lower the 2A energy below the energy of the 1B state at the planar geometry, giving rise to a second fluorescence. In C_{2v} symmetry the transition at the twisted geometry is forbidden. In reality there is an additional distortion that pyramidalizes

TABLE 5: Comparison of Experimental[a] with STEOM-CCSD, CASPT2,[b] and DFT/SCI Vertical Excitation Energies (ΔE in eV), Oscillator Strengths (f), and Dipole Moments (μ in debye) of Planar and Twisted ABN (C_{2v})

		planar				twisted		
		exp	STEOM	CASPT2	DFT/SCI	STEOM	CASPT2	DFT/SCI
S_0	μ	6.6	6.8	6.3	7.2	5.1		5.3
2A	ΔE	4.7	5.1	4.4	5.0	5.1	3.8	4.5
	f		0.55	0.36	0.53	0.00	0.00	0.00
	μ		11.6	12.0	12.8	14.5	15.8	18.1
1B	ΔE	4.2	4.3	4.0	4.3	4.6	4.2	4.7
	f		0.02	0.00	0.03	0.00	0.02	0.00
	μ		7.6	6.1	8.4	5.3	5.2	5.4
1^3A	ΔE		3.3	3.4		3.3	3.3	
1^3B	ΔE		4.1	3.9		4.6	4.1	

[a] References 4, 10, and 39. [b] Reference 12.

TABLE 6: Comparison of Experimental[a] with STEOM-CCSD, CASPT2, and DFT/SCI[c] Vertical Excitation Energies (ΔE in eV), Oscillator Strengths (f), and Dipole Moments (μ in debye) of Planar and Twisted DMABN (C_{2v})

		planar				twisted			
		exptl	STEOM	CASPT2	DFT/SCI	exptl	STEOM	CASPT2	DFT/SCI
S_0	μ	5−7	7.5	7.4	7.9	5−7	5.2	5.8	5.5
2A	ΔE	4.4	4.7	4.4	4.6	3.2	4.0	3.9	3.4
	f	0.72	0.66	0.42	0.66		0.00	0.00	0.00
	μ	11−14	13.5	13.8	16.0	14−20	16.3	15.6	19.3
1B	ΔE[d]	4.0	4.2	4.1	4.1		4.6	5.2	4.5
	f	0.04	0.02	0.01	0.03		0.00	0.00	0.00
	μ	6−11	9.2	7.6	11.5		5.4	5.7	5.9
1^3A	ΔE	2.8	3.2	3.7			3.3	3.7	
1^3B	ΔE		4.0	3.7			4.6	4.4	

[a] References 4, 9, 10, and 42. [b] Reference 12. [c] Reference 15. [d] 2B for DFT/SCI, see text for details.

the nitrogen environment. Then the transition is weakly allowed, and it can fluoresce. Our calculations lend support to this mechanism, and we think it plausible, but inclusion of solvent effects and geometry optimizations of the excited states (possibly in presence of the solvent) would be needed to settle the issue.

Our calculations lend support to the TICT mechanism, but they also argue against other proposed mechanisms to explain the dual fluorescence. The first and second excited state are separated by a distinct energy gap. Even for DMABN, where a small gap is postulated according to Zachariasse et al.,[9,10] a difference in total energy results, which is definitely too large (0.58 eV) to allow a substantial vibronic coupling between the two states. In aminobenzonitrile, the energy gap $\Delta E(S_2-S_1)$ is larger by less than 0.3 eV. We do not find any indication that pseudo Jahn−Teller coupling[9,10] is able to explain the different photophysical properties of ABN compared to DMABN. Also, the differences in the dipole moments are too small to become the decisive factor in a solvent induced state crossing, when both excited states are separated by a relatively large energy gap.

Most importantly, the STEOM-CCSD calculations clearly indicate the difference between ABN and DMABN. In DMABN the excitation energy, and total energy of the charge transfer state is lowered upon twisting the amino group. In ABN this energy is raised upon twisting. This behavior correlates directly with the behavior of ionization energies and electron affinities. In ABN the sum of IP and EA raises by 0.7 eV upon twisting, while in DMABN this energy is lowered by 0.3 eV. This difference between ABN and DMABN is completely due to the difference in ionization potential corresponding to the amino lone pair. In ABN the ionization potential is raised upon twisting, implying a destabilization of the ionized cationic state in which charge is localized on the amino group at the twisted geometry. In contrast for DMABN the methyl groups stabilize the cation, and there is less difference in ionization potential upon twisting.

This simple picture of the process is lost in the CASPT2 calculations. As mentioned above in the CASPT2 calculations it is the excited state in ABN that is lowered upon twisting (although there is found to be a barrier to the twisting motion). We argued above that the CASPT2 results may be suspicious, because of potential difficulties with the description of nitrogen lone pairs. The nature of the lone pair orbital changes completely upon rotation of the amino group, and we definitely consider it a possibility that the behavior of the calculated CASPT2 potential energy curves is artificial. In the CASPT2 calculation a wagging motion of the amino group is considered in addition. This motion lowers the energy of the 2A state in DMABN, while it raises the energy in ABN. This motion is crucial in explaining dual fluorescence from CASPT2 data. In STEOM-CCSD it will be part of the picture, but merely considering the twisting of the amino group already provides a tentative answer. This raises again the question what would happen upon a full geometry optimization of the excited state. It would appear (from the CASPT2 results) that the charge transfer state in ABN is closer to having C_{2v} symmetry than in DMABN. This implies a further lowering of the excited state energy in DMABN, favoring dual fluorescence, while in ABN the picture will not change from the present one: the minimum energy of the 2A state would presumably correspond to a near planar geometry.

4. Discussion and Conclusion

We have presented in this paper a similarity transformed equation-of-motion coupled-cluster study on the organic donor−acceptor compounds ABN and DMABN in order to obtain a closer insight in the photophysics of both compounds by using a method that includes a high level of electron correlation.

In the first part we considered ionization potentials at the IP-EOM-CCSD level which show a markedly different behavior for ABN and DMABN upon twisting the amino group. Whereas the ionization potential corresponding to the nitrogen lone pair

orbital for DMABN is hardly affected by the twisting, the corresponding IP for ABN goes up appreciably. This difference in ionization potential is explained in terms of the electron-donating strength of the CH_3 groups. The stability of the cationic state in ABN is crucially dependent on the conjugation of the nitrogen lone pair orbital and the π framework in order to delocalize the charge. This conjugation is lost upon twisting and this explains the corresponding rise in ionization potential in ABN. In the DMABN cation the charge delocalization is accomplished by the methyl groups, and the stability of the cation depends less on the conjugation effect. We also established that it is crucial to use a correlated method to arrive at the proper description of the cationic states. Koopmans' theorem is inadequate for both the ordering of the states (the stability of cations in which ionization takes place from the nitrogen lone pair orbital is consistently underestimated), while also the change upon twisting is not accurately represented.

Taking into account the lowering of the π^* electron affinity upon twisting in both ABN and DMABN this difference in ionization potential correlates with the behavior of excitation energies upon twisting. Overall the charge transfer state in DMABN is lowered, while this state in ABN increases in energy upon twisting. The TICT explanation of dual fluorescence process is supported by the present calculations, but a more complete study would involve a geometry optimization of the excited states. Also solvent effects are important, but they can alternatively be estimated from experiment. Excitation energies of the charge transfer state change by about 0.2 eV in going from apolar to polar solvents. Therefore we think the effect of geometry optimization will be of major importance.

Secondly, we have compared the calculated absorption spectra of ABN and DMABN to the experimental data and CASPT2[12] and DFT/SCI[15] computations. In general the various methods agree reasonably well. However, surprisingly, the variations in energy upon twisting the amino group show different behavior, in particular for the charge transfer state. In STEOM-CCSD the energy for this state increases upon twisting in ABN while it decreases for DMABN, in accord with the behavior of ionization potentials and electron affinities. This also provides an immediate qualitative picture of the TICT process and the difference between ABN and DMABN. In contrast in previous CASPT2 calculations the reverse was found. A decrease in energy upon twisting for ABN, a slight increase for DMABN. In CASPT2 the wagging motion of the pyramidalization of the amino group has to be invoked to obtain a qualitative picture of the TICT process. It is our estimate, based on previous comparisons between STEOM-CCSD, CASPT2 and EOM-CCSD($\tilde{T}$) that CASPT2 may have difficulties describing the differential correlation in electronic transitions involving lone pair electrons. Therefore we think that the STEOM-CCSD results provide the more accurate picture.

We also compared our results with the recently published DFT/SCI method,[43] which represents another routinely applicable method for calculation of excited state properties, and which is more cost-effective than STEOM-CCSD. DFT/SCI has also been applied to the investigation of the photophysics of DMABN and derivatives.[15] The energetics in DFT/SCI is of STEOM-CCSD quality, however, dipole moments tend to be overestimated. The main experience until now with DFT/SCI concerns low-lying excited states. The behavior of DFT/SCI in the description of complete excitation spectra needs to be examined further. A case in point is the first excited state of B symmetry in twisted DMABN. For both the STEOM-CCSD and CASPT2[12] calculations, this state does not have charge transfer character. In contrast, the DFT/SCI method predicts a highly polar CT state of B symmetry at twisted conformation, energetically closely lying to a nonpolar state of B symmetry. This polar state is not seen at all in the STEOM-CCSD calculations at this low energy. There is little doubt that the ab initio methods yield the proper description of these states and this casts some doubt on the reliability of DFT/SCI for higher excited states, which is related to an often poor description of ionization potentials within the DFT variant of Koopmans' theorem.

Registry Numbers (supplied by author). ABN, 873-74-5; DMABN, 1197-19-9.

Acknowledgment. This work has been supported by the *Fonds zur Förderung der wissenschaftlichen Forschung* (P 11880-CHE) in Austria. We would also like to acknowledge use of computational facilities at the Quantum Theory project, University of Florida, and Stefan Grimme, University of Bonn, Germany, for additional DFT/SCI calculations.

References and Notes

(1) Lippert, E.; Lüder, W. *Advances in Molecular Spectroscopy*, Mangini, A., Ed.; Pergamon Press: Oxford, 1962.
(2) Rettig, W. *Angew. Chem.* **1986**, *98*, 969; *Angew Chem., Int. Ed. Engl.* **1986**, *25*, 971.
(3) Rettig, W. *Top. Curr. Chem.* **1994**, *169*, 253.
(4) Grabowski, Z. R.; Rotkiewicz, K.; Siemiarczuk, A.; Cowley, D. J.; Baumann, W. *Nouv. J. Chim.* **1979**, *3*, 443.
(5) Rotkiewicz, K.; Grellmann, K. H.; Grabowski, Z. R. *Chem. Phys. Lett.* **1973**, *19*, 315.
(6) Weisenborn, P. C. M.; Varma, C. A. G. O.; DeHaas, M. P.; Warmann, J. M. *Chem. Phys. Lett.* **1986**, *129*, 562.
(7) Visser, R. J.; Weisenborn, P. C. M.; Varma, C. A. G. O. *Chem. Phys. Lett.* **1985**, *113*, 330.
(8) Chandross, E. A. *Exciplex*; Gordon, M., Ware, W. R., Eds.; Academic Press: New York, 1975.
(9) Zachariasse, K. A.; von der Haar, T.; Hebecker, A.; Leinhos, U.; Kühnle, W. *Pure Appl. Chem.* **1993**, *65*, 1745.
(10) Schuddeboom, W.; Jonker, S. A.; Warman, J. M.; Leinhos, U.; Kühnle, W.; Zachariasse, K. A. *J. Phys. Chem.* **1992**, *96*, 10809.
(11) Leinhos, U.; Kühnle, W.; Zachariasse, K. A. *J. Phys. Chem.* **1991**, *95*, 2013.
(12) Serrano-Andrés, L.; Merchán, M.; Roos, B. O.; Lindh, R. *J. Am. Chem. Soc.* **1995**, *117*, 3189.
(13) Sobolewski, A. L.; Domcke, W. *Chem. Phys. Lett.* **1996**, *250*, 428.
(14) Sobolewski, A. L.; Domcke, W. *Chem. Phys. Lett.* **1996**, *259*, 119.
(15) Parusel, A. B. J.; Köhler, K.; Grimme, S. *J. Chem. Phys. A* **1998**, *102*, 6297.
(16) Geertsen, J.; Rittby, M.; Bartlett, R. J. *Chem. Phys. Lett.* **1989**, *164*, 57.
(17) Stanton, J. F.; Bartlett, R. J. *J. Chem. Phys.* **1993**, *98*, 7029.
(18) Bartlett, R. J.; Stanton, J. F. *Rev. Comput. Chem.* **1994**, *5*, 65.
(19) DelBene, J. E.; Watts, J. D.; Bartlett, R. J. *J. Chem. Phys.* **1997**, *106*, 6051.
(20) Nooijen, M.; Bartlett, R. J. *J. Chem. Phys.* **1997**, *106*, 6441.
(21) Nooijen, M.; Bartlett, R. J. *J. Chem. Phys.* **1997**, *107*, 6812.
(22) Nooijen, M.; Bartlett, R. J. *J. Chem. Phys.* **1997**, *106*, 6449.
(23) Nooijen, M. *Spectrochim. Acta A* **1998**. In Press.
(24) Woon, D. E.; Dunning, T. H., Jr. *J. Chem. Phys.* **1993**, *98*, 1358.
(25) Kendall, R. A.; Dunning, T. H., Jr.; Harrison, R. J. *J. Chem. Phys.* **1992**, *96*, 6796.
(26) Dunning, T. H., Jr. *J. Chem. Phys.* **1989**, *90*, 1007.
(27) Becke, A. D. *J. Chem. Phys.* **1993**, *98*, 5648.
(28) Stephens, P. J.; Devlin, F. J.; Chabalowski, C. F.; Frisch, M. J. *J. Phys. Chem.* **1994**, *98*, 11623.
(29) Frisch, M. J.; Trucks, G. W.; Schlegel, H. B.; Gill, P. M. W.; Johnson, B. G.; Robb, M. A.; Cheeseman, J. R.; Keith, T.; Petersson, G. A.; Montgomery, J. A.; Raghavachari, K.; Al-Laham, M. A.; Zakrzewski, V. G.; Ortiz, J. V.; Foresman, J. B.; Peng, C. Y.; Ayala, P. Y.; Chen, W.; Wong, M. W.; Andres, J. L.; Replogle, E. S.; Gomperts, R.; Martin, R. L.; Fox, D. J.; Binkley, J. S.; Defrees, D. J.; Baker, J.; Stewart, J. J. P.; Head-Gordon, M.; Gonzalez, C.; Pople, J. A. *Gaussian 94*, Revision B.3; Gaussian, Inc.: Pittsburgh, PA, 1995.
(30) Stanton, J. F.; Gauss, J.; Watts, J. D.; Nooijen, M.; Oliphant, M.; Perera, S. A.; Szalay, P. G.; Lauderdale, W. J.; Gwaltney, S. R.; Beck, S.; Balková, A.; Bernholdt, D. E.; Baeck, K.-K.; Rozyczko, P.; Sekino, H.;

Huber, C.; Bartlett, R. J. *ACESII*; Quantum Theory Project, University of Florida: Gainesville.

(31) Stanton, J. F.; Gauss, J.; Watts, J. D.; Lauderdale, W. J.; Bartlett, R. J. *Int. J. Quantum Chem.* **1991** *526*, 879.

(32) Nooijen, M.; Snijders, J. G. *Int. J. Quantum Chem.* **1993**, *48*, 15.

(33) Stanton, J. F.; Gauss, J. *J. Chem. Phys.* **1995**, *103*, 1064.

(34) Nooijen, M.; Bartlett, R. J. *J. Chem. Phys.* **1995**, *102*, 3629.

(35) LaFemina, J. P.; Duke, C. B.; Paton, A. *J. Chem. Phys.* **1987**, *87*, 2151.

(36) Köhler, G.; Grabner, G.; Rotkiewicz, K. *Chem. Phys.* **1993**, *173*, 275.

(37) Rettig, W.; Dedonder-Lardeaux, C.; Jouvet, C.; Martrenchard-Barra, S.; Szrifiger, P.; Krim, L.; Castano, F. *J. Chim. Phys.* **1995**, *92*, 465.

(38) Rettig, W.; Gleiter, R. *J. Phys. Chem.* **1985**, *89*, 4676.

(39) Gibson, E. M.; Jones, A. C.; Philips, D. *Chem. Phys. Lett.* **1988**, *146*, 270.

(40) Gibson, E. M.; Jones, A. C.; Philips, D. *Chem. Phys. Lett.* **1987**, *136*, 454.

(41) Rechthaler, K.; Parusel, A. B. J. Unpublished results.

(42) Baumann, W.; Bischof, H.; Frohling, J.-C.; Brittinger, C.; Rettig, W.; Rotkiewicz, K. *J. Photochem. Photobiol.* **1992**, *64*, 49.

(43) Grimme, S. *Chem. Phys. Lett.* **1996**, *259*, 128.

(44) Rettig, W.; Suppan, P.; Vauthey, E.; Rotkiewicz, K.; Luboradzki, R.; Suwinska, K. *J. Phys. Chem.* **1993**, *97*, 13500.